Direct functionalization of C–H bonds by electrophilic anions

Jonas Warneke[a,b,c,1], Martin Mayer[a,2], Markus Rohdenburg[d,2], Xin Ma[b,2], Judy K. Y. Liu[b], Max Grellmann[a], Sreekanta Debnath[e], Vladimir A. Azov[f], Edoardo Apra[g], Robert P. Young[g], Carsten Jenne[h], Grant E. Johnson[c], Hilkka I. Kenttämaa[b], Knut R. Asmis[a,1], and Julia Laskin[b,1]

[a]Wilhelm-Ostwald-Institut für Physikalische und Theoretische Chemie, Universität Leipzig, 04103 Leipzig, Germany; [b]Department of Chemistry, Purdue University, West Lafayette, IN 47907; [c]Physical Sciences Division, Pacific Northwest National Laboratory, Richland, WA 99352; [d]Institut für Angewandte und Physikalische Chemie, Fachbereich 2-Biologie/Chemie, Universität Bremen, 28359 Bremen, Germany; [e]Fritz-Haber-Institut der Max-Planck-Gesellschaft, 14195 Berlin, Germany; [f]Department of Chemistry, University of the Free State, 9300 Bloemfontein, South Africa; [g]Environmental Molecular Sciences Laboratory, Pacific Northwest National Laboratory, Richland, WA 99352; and [h]Anorganische Chemie, Fakultät für Mathematik und Naturwissenschaften, Bergische Universität Wuppertal, 42119 Wuppertal, Germany

Edited by Robert H. Crabtree, Yale University, New Haven, CT, and approved August 3, 2020 (received for review March 9, 2020)

Alkanes and $[B_{12}X_{12}]^{2-}$ (X = Cl, Br) are both stable compounds which are difficult to functionalize. Here we demonstrate the formation of a boron–carbon bond between these substances in a two-step process. Fragmentation of $[B_{12}X_{12}]^{2-}$ in the gas phase generates highly reactive $[B_{12}X_{11}]^-$ ions which spontaneously react with alkanes. The reaction mechanism was investigated using tandem mass spectrometry and gas-phase vibrational spectroscopy combined with electronic structure calculations. $[B_{12}X_{11}]^-$ reacts by an electrophilic substitution of a proton in an alkane resulting in a B–C bond formation. The product is a dianionic $[B_{12}X_{11}C_nH_{2n+1}]^{2-}$ species, to which H^+ is electrostatically bound. High-flux ion soft landing was performed to codeposit $[B_{12}X_{11}]^-$ and complex organic molecules (phthalates) in thin layers on surfaces. Molecular structure analysis of the product films revealed that C–H functionalization by $[B_{12}X_{11}]^-$ occurred in the presence of other more reactive functional groups. This observation demonstrates the utility of highly reactive fragment ions for selective bond formation processes and may pave the way for the use of gas-phase ion chemistry for the generation of complex molecular structures in the condensed phase.

electrophilic anions | fragment ion deposition | dodecaborates | alkane functionalization | spectroscopy of reactive intermediates

Understanding and controlling bond breaking and formation processes is central to chemical sciences. Connecting two molecules in a specific manner is a substantial challenge, if the new bond that is formed has to substitute inert bonds in the reagents (1). Synthetic strategies to achieve this goal usually involve complex multistep processes, and the initial bond activation is often based on catalysis using reactive metal centers (2–6). It would be transformative if one could take a stable molecule, break a specific bond, and form a highly reactive undercoordinated binding site, which subsequently is connected to another molecule of choice. This would allow the direct functionalization of abundant feedstock such as saturated hydrocarbons, and "building" of molecular structures in a manner analogous to playing with a molecular modeling kit. Unfortunately, fast quenching of highly reactive intermediates formed by breaking stable bonds makes it difficult to implement this concept using classical condensed-phase chemistry.

Conversely, breaking a stable bond and direct bonding of reactive fragments to inert molecules is quite common in the upper atmospheric layers of planets and moons, where reactions occur in the gas phase at low pressures. For example, in the ionosphere of Saturn's moon Titan, excitation by sunlight or collisions with high-energy particles form reactive molecular fragment ions from organic compounds (7). These fragment ions are able to bind unreactive molecules, forming intermediates that may be subsequently converted into complex organic compounds (8). However, such exoatmospheric reactions lack specificity and, thereby, generate a broad spectrum of products from a mixture of available organic precursors.

Our aim is to use the bond formation principles of ionospheric chemistry in a controlled way for chemical synthesis. This will enable bond formation with unreactive molecular units, which is otherwise difficult to achieve. Chemistry of isolated ions is traditionally studied in the rarefied environment of a mass spectrometer, which somewhat resembles that of the ionosphere and often allows controlled breaking of selected bonds by utilizing an appropriate fragmentation method based on ion-neutral, ion–electron, ion–ion, or ion–photon interactions and subsequent isolation of the reactive fragment ions. Herein, we demonstrate that 1) gas-phase ion chemistry enables covalent bond formation between two molecular units which are both difficult to functionalize: alkanes and highly stable inorganic *closo*-dodecaborate anions; 2) this process occurs through a C–H functionalization mechanism atypical for anions; and 3) products of such reactions can be made amenable to bulk phase characterization using the recently developed high-flux ion soft-landing technique.

The first proof-of-concept experiment, reported here, demonstrates the potential of this approach for the discovery of bond

Significance

Functionalization of unreactive molecules is a significant chemical challenge relevant to the conversion of abundant feedstocks such as alkanes into high-value chemicals. Herein, we demonstrate a new mechanism of alkane functionalization by the substitution of a proton by an anion in an alkyl chain. The reactive anion used for this reaction is generated from a highly stable precursor. The reaction mechanism is established using experimental and computational approaches, and the products are collected in the condensed phase using high-flux mass-selected ion deposition. This paves the way for exploiting the properties of gaseous ions for the generation of complex molecular structures in the condensed phase.

Author contributions: J.W., G.E.J., H.I.K., K.R.A., and J.L. designed research; J.W., M.M., M.R., X.M., J.K.Y.L., M.G., S.D., E.A., and R.P.Y. performed research; C.J. contributed new reagents/analytic tools; J.W., M.M., M.R., X.M., V.A.A., E.A., R.P.Y., C.J., G.E.J., H.I.K., K.R.A., and J.L. analyzed data; J.W. wrote the paper; and V.A.A. performed important literature research.

The authors declare no competing interest.

This article is a PNAS Direct Submission.

[1]To whom correspondence may be addressed. Email: jonas.warneke@uni-leipzig.de, knut.asmis@uni-leipzig.de, or jlaskin@purdue.edu.

[2]M.M., M.R., and X.M. contributed equally to this work.

This article contains supporting information online at https://www.pnas.org/lookup/suppl/doi:10.1073/pnas.2004432117/-/DCSupplemental.

First published September 2, 2020.

formation processes. This development opens the possibility to generate complex molecular structures that are difficult to synthesize using traditional approaches.

The *closo*-dodecaborate anions $[B_{12}X_{12}]^{2-}$ (X = Cl,Br) are well known for their exceptional chemical inertness (9–11). Synthetic approaches for specific B–X functionalization of these anions with organic molecules do not exist but may open broad perspectives for applications, for example, in boron neutron capture therapy and for development of nonlinear optical materials (12–14). Transfer of $[B_{12}X_{12}]^{2-}$ into a mass spectrometer using electrospray ionization (ESI) followed by collision-induced dissociation (CID) generates highly reactive gaseous fragment anions $[B_{12}X_{11}]^-$ (15). Despite the overall negative charge, the undercoordinated boron atom possesses a partial positive charge and is exceptionally electrophilic, as has been demonstrated by the spontaneous binding of noble gases (16, 17). Herein, we describe the reactivity of $[B_{12}Br_{11}]^-$ (**1**) toward alkanes (**2**) by using methane (**2a**) and *n*-hexane (**2b**) as representative model systems. Then, we also extend this reactivity to the condensed phase and to more complex organic molecules (**2c**) by using ion soft landing, see Fig. 1. We focus on the reactivity of $[B_{12}Br_{11}]^-$ in this paper, but additional results summarized in *SI Appendix* demonstrate the equivalent reactivity for $[B_{12}Cl_{11}]^-$. Experimental details are described in *Methods* and in *SI Appendix*, section S1.

Results and Discussion

Gas-Phase Ion Chemistry and Spectroscopy. Ion–molecule reactivity studies of **1** with **2a** and **2b** in the gas phase performed using an ion trap mass spectrometer (Fig. 2*A* and *SI Appendix*, section S2) demonstrate that **1** spontaneously binds to alkanes at room temperature (Eq. **1**).

$$[B_{12}Br_{11}]^-(\mathbf{1}) + C_nH_{2n+2}(\mathbf{2}) \rightarrow [B_{12}Br_{11}C_nH_{2n+2}]^-(\mathbf{3}). \quad [1]$$

Photofragmentation of $[B_{12}Br_{11}CH_4]^-$ **3a** (*SI Appendix*, section S3) or CID of $[B_{12}Br_{11}C_6H_{14}]^-$ **3b** (Fig. 2*B*) did not lead to the formation of the original reagents **1** and **2**. Instead, other dissociation products were formed, indicating that alkanes form strong bonds with **1**. In addition to the reaction product **3**, its water adduct (**4**) (+*m*/*z* 18) was observed. This adduct ion was also observed when **3** was isolated and stored in the ion trap. We attribute this adduct to a reaction of **3** with trace amounts of water present in the instrument. Assuming that the undercoordinated site in **1** is saturated upon reaction with the alkane (Eq. **1**), the formation of **4** (Eq. **2**) indicates the presence of an additional reactive site in **3**, which will be discussed later.

$$[B_{12}Br_{11}C_nH_{2n+2}]^-(\mathbf{3}) + H_2O \rightarrow [B_{12}Br_{11}C_nH_{2n+4}O]^-(\mathbf{4}). \quad [2]$$

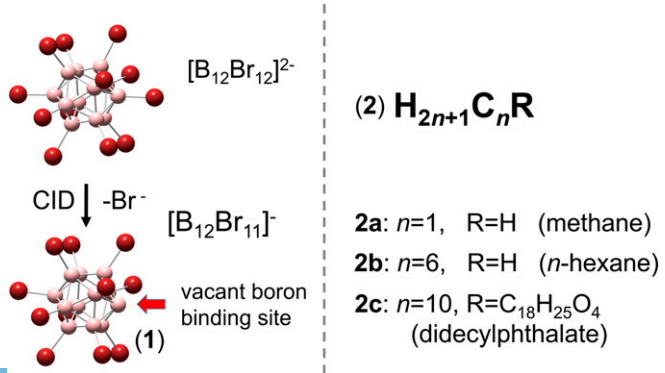

Fig. 1. Reagents and the reactive intermediate used in this study.

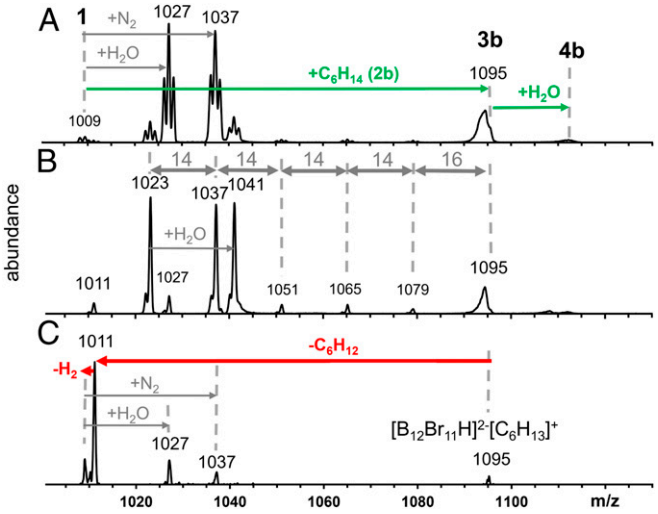

Fig. 2. (*A*) Isolation of anion **1** (*m*/*z* 1009) with an isolation window of *m*/*z* 1.5 followed by reaction for 30 ms with gaseous *n*-hexane **2b** and background gases (N_2, H_2O) in an ion trap mass spectrometer. (*B*) Subsequent CID mass spectrum of the isolated anion **3b** (isolation window of *m*/*z* 1; for more information, see *SI Appendix*, section S2). (*C*) CID of the anion $[B_{12}Br_{11}H]^{2-}[C_6H_{13}]^+$ with the same molecular formula as **3b** but generated upon *n*-hexyl cation transfer from $[N(C_6H_{13})_4]^+$ to $[B_{12}Br_{11}H]^{2-}$.

The formation of **3** cannot be explained by H atom abstraction and carbene formation (18), because the corresponding products ($[B_{12}Br_{11}H]^{-\bullet}$ and $[B_{12}Br_{11}C_nH_{2n}]^-$) were not detected. A detailed reaction scheme is shown in *SI Appendix*, section S2. A classical C–H bond insertion mechanism, as known for metal cations and electron deficient carbenes, requires binding both the carbon and hydrogen to the reactive atom (19). This process can also be excluded, because the reactive boron atom in **1** can only form one covalent bond. In contrast, hydride abstraction from the alkane by **1** would yield a stable, fully substituted *closo*-dodecaborate dianion $[B_{12}Br_{11}H]^{2-}$ which would be electrostatically bound to the $[C_nH_{2n+1}]^+$ cation in the gas phase. The *closo*-dodecaborate anions are known to stabilize alkyl cations (11). The product, $[B_{12}Br_{11}H]^{2-}[C_nH_{2n+1}]^+$, is consistent with the molecular formula of **3** and contains a B–H bond. Two independent experiments were performed to test the structure of the product. Infrared photodissociation (IRPD) spectroscopy of **3a** revealed the presence of vibrational modes characteristic of brominated B_{12} cages but no B–H stretching band around 2,600 cm^{-1} (*SI Appendix*, section S4). Further, we generated $[B_{12}Br_{11}H]^{2-}[C_6H_{13}]^+$, an anion with the same molecular formula as **3b,** in the gas phase using ESI of a salt containing $[B_{12}Br_{11}H]^{2-}$ anions and $[N(C_6H_{13})_4]^+$ cations. Isolation of this ion pair in an ion trap followed by CID produced $[B_{12}Br_{11}H]^{2-}[C_6H_{13}]^+$ via the loss of neutral trihexylamine. The product $[B_{12}Br_{11}H]^{2-}[C_6H_{13}]^+$ showed no reactions with water and a very different CID pattern (15) compared to **3b** (Fig. 2 *B* and *C*). These results indicate that **3** is structurally different from the isobaric ion pair $[B_{12}Br_{11}H]^{2-}[C_nH_{2n+1}]^+$. Therefore, we propose that hydride abstraction is not the predominant reaction pathway.

Since the presence of a B–H bond in the covalent adduct **3** can be ruled out, B–C bond formation is considered. We hypothesize that a C–H bond in the alkane is heterolytically cleaved by **1** in a concerted mechanism, formally generating a proton and a carbanion $[C_nH_{2n+1}]^-$. The carbanion forms a covalent bond with the electrophilic boron atom in **1**, while the proton becomes electrostatically bound to the fully saturated $[B_{12}Br_{11}C_nH_{2n+1}]^{2-}$ dianion to form **3**. This hypothesis is corroborated by computational investigations. Specifically, the potential energy surface

shown in Fig. 3*A* indicates that formation of a collision complex between **2a** and **1** is energetically favored by 84 kJ/mol. The lowest-energy transition state for cleaving a C–H and forming a B–C bond lies 40 kJ/mol below the energy of the separated reactants, making this pathway readily accessible (Fig. 3*A*). The final product **3a** contains an electrostatically bound proton. Theoretical studies of protons electrostatically bound to $[B_{12}X_{12}]^{2-}$ moieties in the gas phase have predicted the location of the proton to be on a Br–Br or Cl–Cl edge (20, 21). This is in agreement with the current investigation. The proton is mobile with respect to edge-to-edge migration that involves relatively small energy barriers (~20 kJ/mol). The thermochemically most favored isomer of **3a** lies 117 kJ/mol below the entrance channel.

The proposed structure of **3a** explains the observed subsequent water addition (Eq. **2**). The reactive site in **3** mentioned before is therefore identified as the electrostatically bound proton. Upon interactions with **3**, a water molecule is readily protonated, resulting in the formation of $[H_3O]^+$ that remains bound to the dianion $[B_{12}Br_{11}C_nH_{2n+1}]^{2-}$. The presence of a hydronium ion in **4a** (Eq. **2**) was confirmed by IRPD spectroscopy (Fig. 3*B*). Specifically, the IRPD spectrum of **4a** reveals characteristic features at 1,580 cm^{-1} (hydronium bending mode) and 1,300 cm^{-1} (hydronium umbrella mode) next to a band at 1,000 cm^{-1} originating from the B_{12} unit, which are strongly indicative of the presence of $[H_3O]^+$ (*SI Appendix*, section S5). However, the unambiguous assignment of the IR bands observed at larger wavenumbers (2,300 cm^{-1} to 3,000 cm^{-1}) is challenging, due to anharmonic and dynamic effects previously reported for water-containing clusters, which can be difficult to predict theoretically (22). Therefore, we also measured the IRPD spectrum of $[B_{12}Br_{12}]^{2-}[H_3O]^+$ generated using published procedures (20), which was found to be almost identical to the spectrum of **4a** (Fig. 3*C*), confirming its assignment.

Our results confirm that the electrophilic closed shell anion **1** is able to substitute a proton in the alkanes **2a** (pK_a of ~50) and **2b** by forming an electrostatically bound complex of the dianion $[B_{12}Br_{11}C_nH_{2n+1}]^{2-}$ and H^+. For many decades, considerable efforts have been dedicated to understanding the details of C–H activation processes using different reagents and conditions. (2, 4, 5, 18, 23–26). Many mechanisms of this important process have been proposed. Proton substitution by several late transition metal complexes resulting in formation of a carbon–metal bond has been investigated. (2, 4, 24, 27). There are many open-shell metal and metal oxide cluster ions known which can activate the C–H bond of methane in the gas phase at thermal collision energies. (26) Thermal reactions between methane and closed-shell anions are scarce. Nevertheless, this reaction has been reported for $[AuTi_3O_7]^-$, which contains an electrophilic gold atom. (28) Heterolytic C–H cleavage in methane on $[AuTi_3O_7]^-$ was discussed in terms of Lewis acid–base pairs (LABP) and special properties of gold caused by the strong relativistic effects on this element. The LABP model is also often used to explain the activation of strong bonds by reactive boron centers (29, 30). However, it does not seem to be applicable here, since the lone pairs in **1** have an exceptionally weak Lewis base character, and protonated $[B_{12}X_{12}]^{2-}$ anions are among the strongest Brønsted acids known (10). The reactivity of **1** may be better rationalized by 1) binding of a carbanion to the highly electrophilic boron site and 2) Coulomb stabilization of the resulting ion pair. Ion **3** exhibits the exceptional property of acting as a strong donor for a proton previously abstracted from an alkane.

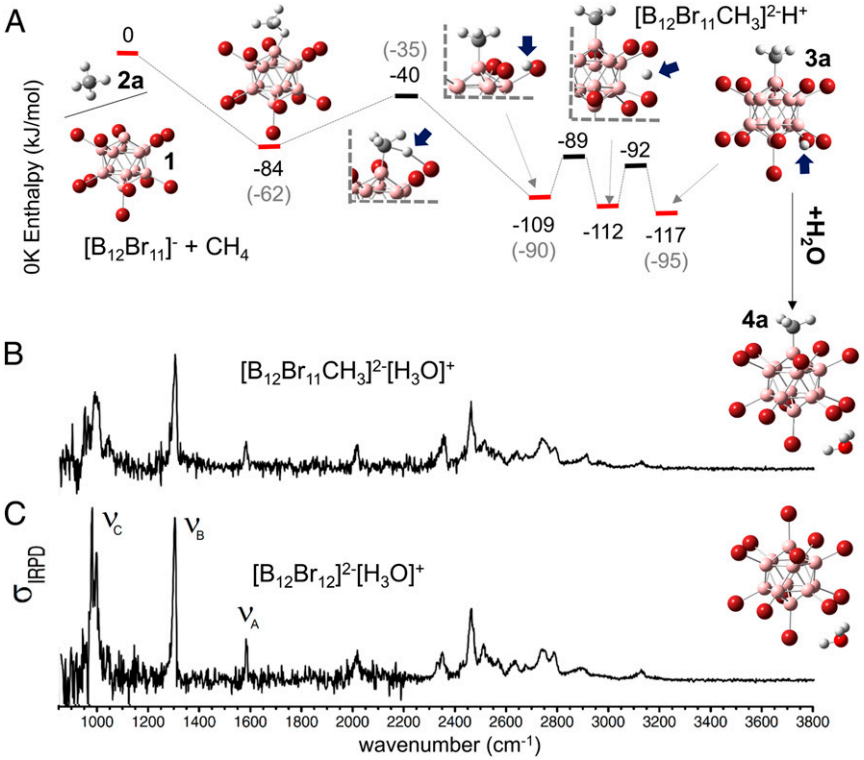

Fig. 3. (*A*) Reaction path including the energies (in kilojoules per mole) and structures of minima (red) and transition states (black) for the reaction of **1** with methane as calculated at the B3LYP-D3/6-311++G(2d,2p) level of theory. A blue arrow marks the abstracted proton (we note that a strong kinetic isotope effect for C-H cleavage should take place if CD_4 was used). Key geometries were reoptimized at the SCS-MP2/ccpVTZ level of theory (energies in gray numbers in parentheses). For some of the structures, only the reaction-relevant part is outlined using gray dashed lines. (*B*) IRPD spectrum of **4a**. (*C*) IRPD spectrum of $[B_{12}Br_{12}]^{2-}[H_3O]^+$ for comparison (ν_A, H_3O^+ bending mode; ν_B, H_3O^+ umbrella mode; ν_C, B–Br stretching vibrations, coupled to B_{12}-cage deformation modes). The depicted spectra consist of two parts joined together at 2,200 cm^{-1}.

Ion Deposition Experiments. The reaction discussed herein, first discovered in the gas phase, may also be employed for the preparation of new compounds in the condensed phase. For this, ion soft landing (31) is employed, which enables the controlled deposition of mass-selected ions on surfaces. In recent years, brighter (higher ion flux) ionization sources with the potential to produce macroscopic quantities of condensed-phase material from mass-selected ions have been developed (32–37). Examples of the generation of macroscopic amounts of material from fragment ions, however, are very scarce. One notable example is the generation of a polymeric carbon material from the deposition of the fullerene fragment C_{58}^+ (38). In our experiments, we used high flux ESI-coupled ion soft landing to deposit a reactive fragment and accumulated the products (Fig. 4*A*). Recently, we showed the formation of condensed layers on surfaces by the deposition of mass-selected $[B_{12}X_{12}]^{2-}$ anions (39). Phthalate molecules (including **2c** as a dominant species), which were present in the background of the instrument, accumulated with the anions during the deposition process. ESI mass spectrometry (ESI-MS) analysis of the deposited layers revealed the presence of intact $[B_{12}X_{12}]^{2-}$ ions in negative ion mode and accumulated phthalate molecules, which were detected as Na^+ adducts in positive ion mode. Upon in-source CID of gas-phase $[B_{12}Br_{12}]^{2-}$, **1** was generated and mass selected in our soft-landing instrument. Around 5×10^{14} anions **1** were deposited in the presence of phthalates on a gold surface which was coated by a chemically inert fluorinated alkane thiol self-assembled monolayer. The substrate was removed from the soft-landing instrument. Condensed matter with a spot size of roughly 3 mm × 3 mm was optically visible on the surfaces (see images in *SI Appendix*, section S6). The deposited layer was dissolved in methanol, and the resulting solution was analyzed using ESI-MS. Remarkably, (−) ESI-MS analysis of the anions in the layer revealed the presence of dianions, although a singly charged anion was mass-selected and deposited. The special electrophilic nature of $[B_{12}Br_{11}]^-$ prevents deposited ions from neutralization but instead drives reactions, which recover the stable doubly charged configuration of the precursor. Each dianion corresponds to a phthalate derivative (compare Fig. 4 *B* and *C*) in which a proton is substituted by a $[B_{12}Br_{11}]^-$ anion. For example, phthalates with decyl chains ($C_{28}H_{46}O_4$) were detected as $[B_{12}Br_{11}C_{28}H_{45}O_4]^{2-}$ (**3c**–H^+). While, in the gas phase, the substituted proton remains electrostatically bound to the dianion, it can be readily released in the condensed phase and is not bound to the dianion during ESI-MS analysis of the deposited layer. CID of this product (Fig. 4*D*) results in the elimination of the aromatic moiety of the pthalate, generating a fragment ion at *m/z* 574, in which **1** is bound to an alkyl chain of the phthalate. The fragmentation pattern of this ion at *m/z* 574 (Fig. 4*E*) resembles the CID pattern of negatively charged primary fatty acids (20) indicating that **1** is preferentially bound to a primary C atom of the alkyl chain. This observation is consistent with the lower energy barrier calculated for proton substitution at a primary C atom in comparison to a secondary C atom of alkyl chains (see details in *SI Appendix*, section S6). Although phthalates contain several functional groups which may act as reaction partners for **1** during the deposition process, **1** has preferentially reacted with inert alkyl groups under these experimental conditions.

Selective binding of a strong electrophile to the alkyl chain in the phthalate rather than the nucleophilic ester groups or the aromatic moiety is remarkable. Attaching **1** to the carbonyl oxygen atom is calculated to be more energetically favorable by ∼150 kJ/mol than proton substitution in the gas phase (*SI Appendix*, section S6). The observed preference for the proton substitution reaction in the layer may be attributed to both kinetic effects and differences between the gas- and condensed-phase thermochemistry of the competing reactions. Polar nucleophiles with a significant partial negative charge in their reactive sites are likely oriented away from the anion, whereas the reactive electrophilic site in **1** may be more accessible to less polar groups such as alkyl chains. It is reasonable to assume that phthalates accumulated at the layer's interface orient the alkyl chains toward the vacuum side, while polar ester groups are oriented toward the ion-rich bulk phase. Such molecular orientation can cause the kinetic hindrance for the reaction of ester oxygens with the deposited reactive ions **1**. In addition, a strong thermodynamic stabilization of the dianionic product and the proton is expected in the deposited layer, due to

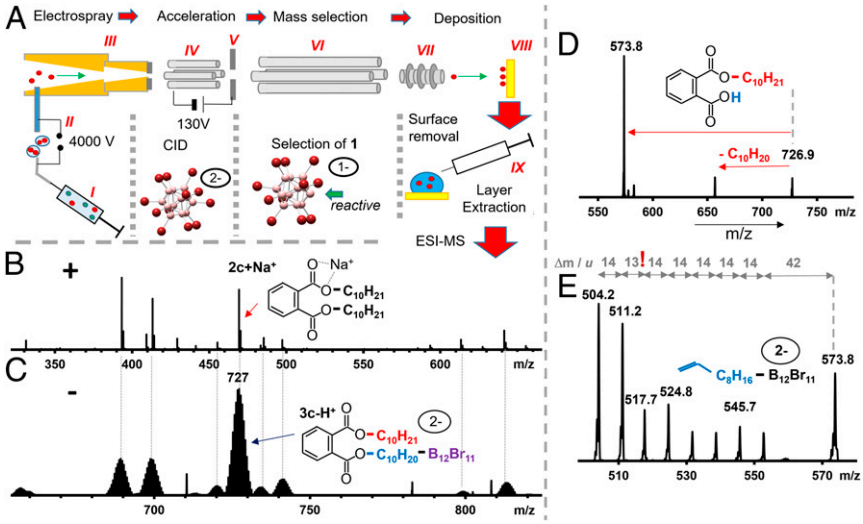

Fig. 4. (*A*) Schematic of the ion soft-landing instrument. ESI source (*I*); heated inlet (*II*); dual ion-funnel system (*III*); collision quadrupole for ion collimation, cooling, and CID (*IV*); and quadrupole mass filter (*VI*) for mass selection of ions (*m/z* ± 10), which were focused by einzel lenses (*VII*) and delivered to a gold surface covered by an alkane thiol self-assembled monolayer (*VIII*). The experimental details are provided in *SI Appendix*, section S6. Voltage gradient between the DC offset of *IV* and conductance limit *V* determines the ion kinetic energy and, thereby, the degree of ion fragmentation. The deposited material was extracted into methanol and analyzed (*IX*). (*B*) (+)ESI mass spectrum of organic molecules present in the vacuum chamber after accumulation on surfaces. For assignments, see *SI Appendix*, section S6. (*C*) (−)ESI mass spectrum of the sample prepared by deposition of **1**, showing the $[B_{12}Br_{11}C_{28}H_{45}O_4]^{2-}$ anion at *m/z* 727; for information on the other products, see *SI Appendix*, section S6. (*D*) Single *m/z*-unit isolation and CID of $[B_{12}Br_{11}C_{28}H_{45}O_4]^{2-}$ (*m/z* 727). (*E*) CID of the isolated fragment ion of *m/z* 574.

short- and long-range electrostatic interactions between multiple counterions in the bulk phase as well as solvation effects. The contribution of these condensed phase effects cannot be evaluated using gas-phase models.

Conclusion

In this article, we demonstrate the preparative potential of gaseous fragment ions. Formation of complex molecules with such ions is usually considered to be relevant only in uncontrolled ionospheric processes. In our approach, we mass select a targeted fragment ion, thus obtaining one reagent with a desirable reactive character. Products of the reactions with this fragment ion may be accumulated on surfaces using advanced ion soft-landing methods. The proof-of-concept case discussed herein demonstrates the ability to interconnect two unreactive substances, dodecaborate ions and alkyl moieties, using a "fragmentation–addition" sequence: generation of the reactive fragment $[B_{12}X_{11}]^-$ by CID in the gas phase followed by its reaction with a nonactivated hydrocarbon chain by proton substitution. This reaction results in a formal substitution of the C–H and B–X bonds in the reagents by a new B–C bond. The highly reactive $[B_{12}X_{11}]^-$ showed an unexpected selectivity toward reactions with alkyl groups in the presence of more reactive ester groups during ion soft-landing experiments. Along with the development of high-flux ion soft-landing instrumentation, these insights into the previously unknown bond formation processes may be used to generate molecular structures in the condensed phase using reactive gaseous fragment ions.

Methods

Reaction with Hexane and CID Experiments. Ion–molecule reactions of $[B_{12}Br_{11}]^-$ and *n*-hexane were studied in a Thermo LTQ linear quadrupole ion trap mass spectrometer at Purdue University, coupled with a homebuilt reagent mixing manifold for the introduction of neutral *n*-hexane into the ion trap. $[(NEt_4)_2][B_{12}X_{12}]$ in methanol was introduced into the gas phase via negative-mode ESI. Fragmentation of mass-selected ions was performed using ion trap CID. More details of the experimental settings and conditions can be found in *SI Appendix*.

IRPD. The IRPD spectra were measured using the Leipzig cryogenic ion trap triple mass spectrometer described elsewhere (40, 41). $[B_{12}Br_{12}]^{2-}$ and $[B_{12}Br_{11}]^-$ anions were produced via skimmer CID from precursor ions formed using a nanospray ion source with a 0.1-mmol/L solution of $[B_{12}Br_{12}][HN(C_2H_5)_3]_2$ in acetonitrile. The ions were collimated in a radio frequency ion guide filled with different buffer gases at room temperature in order to form the respective adducts (H_2O, CH_4). After mass selection, the ions were guided into the ion trap, which was filled with gas mixtures 80% He/20% N_2 or 99% He/1% CO buffer gas and held at temperatures of around 43 K, promoting the formation of weakly bound ion–N_2 or ion–CO messenger complexes. The ions were focused into the center of the extraction region of an orthogonally mounted reflectron time-of-flight (ToF) tandem photofragmentation mass spectrometer, where they were irradiated by tunable IR radiation from an Nd:YAG laser-pumped OPO/OPA/$AgGaSe_2$ laser system. When resonant with a rovibrational transition, the initially internally cold messenger-tagged parent ion absorbs an IR photon, eventually leading to a change in the ion's *m/z* ratio due to loss of the N_2 messenger molecule, which is then detected by ToF MS. Technical details are described in *SI Appendix*.

Photofragmentation. The infrared multiple photon photodissociation (42–44) experiments were carried out with another ion trap tandem mass spectrometer described previously (45, 46). Irradiation is performed with an intense and widely tunable IR pulse from the Fritz Haber Institute Free-Electron Laser (47). Technical details are described in *SI Appendix*.

Computational Investigations. Calculations were performed using the Gaussian09, rev. D.01, and the NWChem program packages. Details on all methods are given in *SI Appendix*.

Synthesis. $[NEt_3H]_2[B_{12}X_{12}]$ (X = Cl, Br) was prepared according to previously reported literature procedures (48, 49).

Ion Soft Landing. The setup of the used ion soft-landing instrument and its technical details were described previously (50). The ion source capable of high ion currents which allows generation of condensed-phase material layers has been described before (33). Details of the experimental settings, including applied voltages to all components of the system and background pressures, are described in *SI Appendix*. The deposition target was prepared by carefully cleaning the gold surface and self-assembly of a monolayer of 1H,1H,2H,2H-perfluorodecanethiol. Details of the preparation process are described in *SI Appendix*.

Data Availability. All study data are included in the article and *SI Appendix*.

ACKNOWLEDGMENTS. J.W. acknowledges a Feodor Lynen fellowship of the Alexander von Humboldt Foundation and a Freigeist fellowship from the Volkswagen Foundation. A portion of the research was performed using Environmental Molecular Sciences Laboratory (EMSL), a Department of Energy (DOE) Office of Science User Facility sponsored by the Office of Biological and Environmental Research. J.L. and G.E.J. acknowledge support from the DOE's Office of Science, Office of Basic Energy Sciences, Division of Chemical Sciences, Geosciences and Biosciences. X.M., J.K.Y.L., and H.I.K. acknowledge Purdue Research Foundation (Grant 60000025). K.R.A. acknowledges instrumental support from the Fritz Haber Institute of the Max Planck Society. M.G. thanks Harald Knorke and Sebastian Kawa (University of Leipzig) for technical support with one experiment, and J.W. thanks Prof. Kirsten Zeitler (University of Leipzig) for some helpful discussions.

1. S. Murai *et al.*, *Activation of Unreactive Bonds and Organic Synthesis*, (Springer, 1999).
2. B. G. Hashiguchi, S. M. Bischof, M. M. Konnick, R. A. Periana, Designing catalysts for functionalization of unactivated C-H bonds based on the CH activation reaction. *Acc. Chem. Res.* **45**, 885–898 (2012).
3. H. Schwarz, S. Shaik, J. Li, Electronic effects on room-temperature, gas-phase C-H bond activations by cluster oxides and metal carbides: The methane challenge. *J. Am. Chem. Soc.* **139**, 17201–17212 (2017).
4. A. E. Shilov, G. B. Shul'pin, Activation of C–H bonds by metal complexes. *Chem. Rev.* **97**, 2879–2932 (1997).
5. H. Schwarz, How and why do cluster size, charge state, and ligands affect the course of metal-mediated gas-phase activation of methane? *Isr. J. Chem.* **54**, 1413–1431 (2014).
6. C. Geng, J. Li, T. Weiske, H. Schwarz, Complete cleavage of the N≡N triple bond by Ta_2N^+ via degenerate ligand exchange at ambient temperature: A perfect catalytic cycle. *Proc. Natl. Acad. Sci. U.S.A.* **116**, 21416–21420 (2019).
7. J. H. Waite Jr. *et al.*, The process of tholin formation in Titan's upper atmosphere. *Science* **316**, 870–875 (2007).
8. A. Li, F. P. M. Jjunju, R. G. Cooks, Nucleophilic addition of nitrogen to aryl cations: Mimicking Titan chemistry. *J. Am. Soc. Mass Spectrom.* **24**, 1745–1754 (2013).
9. C. Knapp, "Weakly coordinating anions: Halogenated borates and dodecaborates" in *Comprehensive Inorganic Chemistry II*, J. Reedijk, K. Poeppelmeier, Eds. (Elsevier, Amsterdam, The Netherlands, 2013), Vol. 1, pp. 651–679.
10. A. Avelar, F. S. Tham, C. A. Reed, Superacidity of boron acids $H_2(B_{12}X_{12})$ (X = Cl, Br). *Angew. Chem. Int. Ed.* **48**, 3491–3493 (2009).
11. C. Bolli *et al.*, Synthesis, crystal structure, and reactivity of the strong methylating agent $Me_2B_{12}Cl_{12}$. *Angew. Chem. Int. Ed.* **49**, 3536–3538 (2010).
12. N. S. Hosmane, *Boron Science: New Technologies and Applications*, (CRC, 2012).
13. M. F. Hawthorne, A. Maderna, Applications of radiolabeled boron clusters to the diagnosis and treatment of cancer. *Chem. Rev.* **99**, 3421–3434 (1999).
14. C. D. Entwistle, T. B. Marder, Boron chemistry lights the way: Optical properties of molecular and polymeric systems. *Angew. Chem. Int. Ed.* **41**, 2927–2931 (2002).
15. J. Warneke, T. Dülcks, C. Knapp, D. Gabel, Collision-induced gas-phase reactions of perhalogenated closo-dodecaborate clusters—A comparative study. *Phys. Chem. Chem. Phys.* **13**, 5712–5721 (2011).
16. M. Rohdenburg *et al.*, Superelectrophilic behavior of an anion demonstrated by the spontaneous binding of noble gases to $[B_{12}Cl_{11}]^-$. *Angew. Chem. Int. Ed.* **56**, 7680–7985 (2017).
17. M. Mayer *et al.*, Rational design of an argon-binding superelectrophilic anion. *Proc. Natl. Acad. Sci. U.S.A.* **116**, 8167–8172 (2019).
18. D. Schröder, H. Schwarz, Gas-phase activation of methane by ligated transition-metal cations. *Proc. Natl. Acad. Sci. U.S.A.* **105**, 18114–18119 (2008).
19. D. H. Ess, W. A. Goddard, R. A. Periana, Electrophilic, ambiphilic, and nucleophilic C–H bond activation: Understanding the electronic continuum of C–H bond activation through transition-state and reaction pathway interaction energy decompositions. *Organometallics* **29**, 6459–6472 (2010).
20. C. Jenne, M. Keßler, J. Warneke, Protic anions $[H(B_{12}X_{12})]$- (X = F, Cl, Br, I) that act as Brønsted acids in the gas phase. *Chem. Eur. J.* **21**, 5887–5891 (2015).
21. L. Lipping *et al.*, Superacidity of closo-dodecaborate-based Brønsted acids: A DFT study. *J. Phys. Chem. A* **119**, 735–743 (2015).
22. K. R. Asmis *et al.*, Gas-phase infrared spectrum of the protonated water dimer. *Science* **299**, 1375–1377 (2003).
23. X.-S. Xue, P. Ji, B. Zhou, J.-P. Cheng, The essential role of bond energetics in C-H activation/functionalization. *Chem. Rev.* **117**, 8622–8648 (2017).

24. J. Sommer, J. Bukala, Selective electrophilic activation of alkanes. *Acc. Chem. Res.* **26**, 370–376 (1993).
25. I. Akhrem, A. Orlinkov, Polyhalomethanes combined with Lewis acids in alkane chemistry. *Chem. Rev.* **107**, 2037–2079 (2007).
26. Y.-X. Zhao, Z.-Y. Li, Y. Yang, S.-G. He, Methane activation by gas phase atomic clusters. *Acc. Chem. Res.* **51**, 2603–2610 (2018).
27. J. Oxgaard, W. J. Tenn, R. J. Nielsen, R. A. Periana, W. A. Goddard, Mechanistic analysis of iridium heteroatom C–H activation: Evidence for an internal electrophilic substitution mechanism. *Organometallics* **26**, 1565–1567 (2007).
28. Y.-X. Zhao *et al*., Methane activation by gold-doped titanium oxide cluster anions with closed-shell electronic structures. *Chem. Sci.* **7**, 4730–4735 (2016).
29. Q. Chen *et al*., Thermal activation of methane by vanadium boride cluster cations VB_n^+ (n = 3-6). *Phys. Chem. Chem. Phys.* **20**, 4641–4645 (2018).
30. Z. Huang *et al*., Boron: Its role in energy related research and applications. *Angew. Chem. Int. Ed.* **59**, 8800–8816 (2020).
31. V. Franchetti, B. H. Solka, W. E. Baitinger, J. W. Amy, R. G. Cooks, Soft landing of ions as a means of surface modification. *Int. J. Mass Spectrom.* **23**, 29–35 (1977).
32. J. Laskin, G. E. Johnson, J. Warneke, V. Prabhakaran, From isolated ions to multilayer functional materials using ion soft landing. *Angew. Chem. Int. Ed.* **57**, 16270–16284 (2018).
33. K. D. D. Gunaratne *et al*., Design and performance of a high-flux electrospray ionization source for ion soft landing. *Analyst* **140**, 2957–2963 (2015).
34. C. Yin, E. Tyo, K. Kuchta, B. von Issendorff, S. Vajda, Atomically precise (catalytic) particles synthesized by a novel cluster deposition instrument. *J. Chem. Phys.* **140**, 174201 (2014).
35. R. E. Palmer, L. Cao, F. Yin, Note: Proof of principle of a new type of cluster beam source with potential for scale-up. *Rev. Sci. Instrum.* **87**, 046103 (2016).
36. M. Pauly *et al*., A hydrodynamically optimized nano-electrospray ionization source and vacuum interface. *Analyst* **139**, 1856–1867 (2014).
37. P. V. Menezes *et al*., Bombardment induced ion transport—Part II. Experimental potassium ion conductivities in borosilicate glass. *Phys. Chem. Chem. Phys.* **13**, 20123–20128 (2011).
38. A. Böttcher *et al*., Solid C58 films. *Phys. Chem. Chem. Phys.* **7**, 2816–2820 (2005).
39. J. Warneke *et al*., Self-organizing layers from complex molecular anions. *Nat. Commun.* **9**, 1889 (2018).
40. N. Heine, K. R. Asmis, Cryogenic ion trap vibrational spectroscopy of hydrogen-bonded clusters relevant to atmospheric chemistry. *Int. Rev. Phys. Chem.* **34**, 1–34 (2015).
41. N. Heine, K. R. Asmis, Cryogenic ion trap vibrational spectroscopy of hydrogen-bonded clusters relevant to atmospheric chemistry. *Int. Rev. Phys. Chem.* **35**, 507 (2016).
42. J. G. Black, E. Yablonovitch, N. Bloembergen, S. Mukamel, Collisionless multiphoton dissociation of SF_6: A statistical thermodynamic process. *Phys. Rev. Lett.* **38**, 1131–1134 (1977).
43. E. R. Grant, P. A. Schulz, A. S. Sudbo, Y. R. Shen, Y. T. Lee, Is multiphoton dissociation of molecules a statistical thermal process? *Phys. Rev. Lett.* **40**, 115–118 (1978).
44. V. N. Bagratashvili, V. S. Letokhov, A. A. Makarov, E. A. Ryabov, Multiple-photon infrared laser photophysics and photochemistry. I. *Laser Chem.* **1**, 211–342 (1983).
45. D. J. Goebbert, G. Meijer, K. R. Asmis, T. Iguchi, K. Watanabe, 10 K ring electrode trap—Tandem mass spectrometer for infrared spectroscopy of mass selected ions. *AIP Conf. Proc.* **1104**, 22–29 (2009).
46. D. J. Goebbert, T. Wende, R. Bergmann, G. Meijer, K. R. Asmis, Messenger-tagging electrosprayed ions: Vibrational spectroscopy of suberate dianions. *J. Phys. Chem. A* **113**, 5874–5880 (2009).
47. W. Schöllkopf *et al*., The new IR and THz FEL facility at the Fritz Haber Institute in Berlin. *Proc. SPIE* **9512**, 95121L (2015).
48. V. Geis, K. Guttsche, C. Knapp, H. Scherer, R. Uzun, Synthesis and characterization of synthetically useful salts of the weakly-coordinating dianion $[B_{12}Cl_{12}]^{2-}$. *Dalton Trans.* **15**, 2687–2694 (2009).
49. I. Tiritiris, T. Schleid, Die Kristallstrukturen der Dicaesium-Dodekahalogeno-closo-Dodekaborate $Cs_2[B_{12}X_{12}]$ (X = Cl, Br, I) und ihrer Hydrate. *Z. Anorg. Allg. Chem.* **630**, 1555–1563 (2004).
50. Q. Hu, P. Wang, P. L. Gassman, J. Laskin, In situ studies of soft- and reactive landing of mass-selected ions using infrared reflection absorption spectroscopy. *Anal. Chem.* **81**, 7302–7308 (2009).